

Regular paper

Spectroscopic characterization of reaction centers of the (M)Y210W mutant of the photosynthetic bacterium *Rhodobacter sphaeroides*

Susana Shochat¹, Thomas Arlt², Christof Francke¹, Peter Gast¹, Paula I. van Noort¹, Stephan C. M. Otte¹, Hans P. M. Schelvis¹, Stefan Schmidt², Erik Vijgenboom³, Jacobien Vrieze¹, Wolfgang Zinth⁴ and Arnold J. Hoff¹

¹Department of Biophysics, Huygens Laboratory, Leiden University, P.O. Box 9504, 2300 RA Leiden, The Netherlands; ²Technische Universität München, Physik Department E 11, James Franck Str., 85748 Garching, Germany; ³Department of Chemistry, Gorlaeus Laboratory, Leiden University, P.O. Box 9502, 2300 RA Leiden, The Netherlands; ⁴Ludwig-Maximilians-Universität München, Institut für Medizinische Optik, Barbarastr. 16, 80797 München, Germany

Received 15 July 1993; accepted in revised form 7 December 1993

Key words: absorption spectrum, ADMR, charge separation, fluorescence spectrum, reaction center, mutant

Abstract

The tyrosine-(M)210 of the reaction center of *Rhodobacter sphaeroides* 2.4.1 has been changed to a tryptophan using site-directed mutagenesis. The reaction center of this mutant has been characterized by low-temperature absorption and fluorescence spectroscopy, time-resolved sub-picosecond spectroscopy, and magnetic resonance spectroscopy. The charge separation process showed bi-exponential kinetics at room temperature, with a main time constant of 36 ps and an additional fast time constant of 5.1 ps. Temperature dependent fluorescence measurements predict that the lifetime of P* becomes 4–5 times slower at cryogenic temperatures. From EPR and absorbance-detected magnetic resonance (ADMR, LD-ADMR) we conclude that the dimeric structure of P is not significantly changed upon mutation. In contrast, the interaction of the accessory bacteriochlorophyll B_A with its environment appears to be altered, possibly because of a change in its position.

Abbreviations: ADMR – absorbance-detected magnetic resonance; LDAO – N, N dimethyl dodecyl amine-N-oxide; RC – reaction center; LD-ADMR – linear-dichroic absorbance-detected magnetic resonance; P – primary donor; B – accessory bacteriochlorophyll; Φ – bacteriopheophytin

Introduction

The primary reactions in bacterial photosynthesis generate chemical energy by a charge separation across a membrane-bound pigment-protein complex, the reaction center (RC). The X-ray structure of the RC of *Rhodospseudomonas viridis* (Michel and Deisenhofer 1986) and *Rhodobacter (Rb.) sphaeroides* R-26 (Allen et al. 1987b) has been solved. It shows that the electron transfer

cofactors are arranged in two branches, A and B, related by a pseudo-C₂ symmetry. The axis of symmetry runs from a dimer of bacteriochlorophyll (BChl) molecules (the primary electron donor, P), at the periplasmic side of the membrane, to an iron atom at the cytoplasmic side. Each branch contains, in addition to one BChl of P, a BChl molecule, located near P (B_A and B_B), a bacteriopheophytin molecule (Φ_A and Φ_B) and a quinone (Q_A and Q_B). Spectroscopic studies

have revealed that electron transfer proceeds only through chain A (reviewed in Kirmaier and Holten 1987).

The cofactors are embedded in a polypeptide complex comprising three subunits (L, M and H). The cofactor chromophores of the active branch (A), and Q_B are associated with the L subunit, while those of the inactive branch (B) and Q_A are associated with the M subunit; the H subunit caps the L and M unit at the quinone sites.

Several amino acids in the vicinity of the cofactors break the symmetry of the complex. It has been suggested that these amino acids play a role in both the unidirectionality (only one active branch) and the highly efficient electron transfer. They may, for example, affect the energy levels of the electron transfer components or the coupling between the different intermediates.

One of the most striking symmetry-breaking residues is tyrosine (M)Y210, which, although part of the M subunit, is located very close to P, B_A , and Φ_A . This residue is conserved in *Rb. capsulatus*, *Rb. sphaeroides*, *Rhodospirillum rubrum* and *Rhodopseudomonas viridis* (Williams et al. 1986). The symmetry-related amino acid in the L polypeptide is phenylalanine at position L181. In *Chloroflexus aurantiacus*, the tyrosine is replaced by leucine (Shiozawa et al. 1989). Charge separation in this bacterium is more than two times slower than in the other bacteria mentioned (Becker et al. 1991, Hamm et al. 1993). Calculations of the electrostatic energy of the reactants involved in charge separation, suggest that the interaction of P and B_A with the polar tyrosine, (M)Y210, lowers the energy of the state $P^+B_A^-$, rendering electron transfer through the A-branch more favorable than that along the B-branch (Parson et al. 1990).

To understand the role of (M)Y210, site-directed mutagenesis techniques have been used to change this residue to phenylalanine (Gray et al. 1990, Nagarajan et al. 1990, Finkle et al. 1990), leucine (Gray et al. 1990, Finkle et al. 1990) and isoleucine (Nagarajan et al. 1990) in *Rb. sphaeroides*, and to phenylalanine, histidine and threonine in *Rb. capsulatus* (Chan et al. 1991). Except for the histidine (which is aromatic and polar like the tyrosine), it was found that in all cases the rate of charge separation was lower in

the mutants than in the wild type, indicating that (M)Y210 plays an important role in the initial electron transfer. Extensive research has been carried out to characterize the mutants mentioned. Considering the charge-separation rate in different mutants of *Rb. capsulatus*, Chan et al. (1991) concluded that both the hydroxyl group and the aromatic ring of the tyrosine are important for efficient electron transfer through the A-branch. Using Raman spectroscopy, Mattioli et al. (1991) concluded that the tyrosine is not hydrogen bonded to P, contrary to a suggestion based on the X-ray structure (Allen et al. 1987a). Thus, a direct interaction with P seems to be excluded. Possibly, the phenolic residue acts on electron transfer by influencing the polarity of the electrostatic environment of P. Nagarajan et al. (1990) performed studies on the temperature dependence of the rate of charge separation in two mutants of *Rb. sphaeroides*. Their results suggest that the mutations indeed raise the energy level of $P^+B_A^-$, making the initial electron transfer reaction thermally activated at room temperature.

In the course of CP/MAS NMR experiments on ^{13}C -tyrosine labelled RCs of *Rb. sphaeroides* R-26 (Fischer et al. 1992), it was decided to replace (M)Y210 with another amino acid for the purpose of peak assignment. Tryptophan was chosen because in principle it allows double-labelling (^{13}C , ^{15}N) experiments. In this communication we report on the physico-chemical properties of the (M)Y210W mutant, characterizing its RC by low-temperature absorption and fluorescence spectroscopy, time-resolved absorbance-difference spectroscopy and magnetic resonance spectroscopy, comparing the results with those reported for other (M)Y210 mutants. Part of this work has appeared in preliminary form (Shochat et al. 1992).

Materials and methods

The restriction endonucleases BamHI, Sall and XhoI were obtained from Amersham Corporation. Kanamycin and tetracycline were from Sigma. The deletion mutant of *Rb. sphaeroides* 2.4.1(ΔLM1), the expression vector, which is a broad host range plasmid pRK404 containing the

puf operon (pRKNEB1), and *Escherichia (E.) coli* S17-1 were made available by Prof. G. Feher (Paddock et al. 1989). Q-sepharose and DEAE sephacel were obtained from Pharmacia; N, N dimethyl dodecyl amine-N-oxide (LDAO) from Fluka Chemie.

The *Rb. sphaeroides* deletion strain complemented with the plasmid bearing wild type or mutated genes was grown semi-aerobically in the dark, on rich medium, in the presence of kanamycin (25 mg/ml) and tetracycline (2.5 mg/ml) (Paddock et al. 1989).

The mutation was incorporated into the gene using a synthetic oligonucleotide carrying the changed codon TAC(try) \rightarrow ACC(trp). The 1 Kb Sall-BamHI fragment, containing the puf M gene, was cloned into the bacteriophage M13 mp19. The Sall-BamHI fragment was isolated from the pRKENB1, which is a derivative of the pRKGln (Paddock et al. 1989) with a BamHI site created downstream from puf M. The M13 clone was used as a template for site-directed mutagenesis according to Kunkel (1987). Sequence analysis confirmed that only this mutation was present. The mutated gene was re-cloned in the expression vector pRKENB1 as a XhoI-BamHI fragment and was transformed into *E. coli* S17-1. This *E. coli* strain carries the genes necessary for plasmid transfer via conjugation. It was then mated with the deletion mutant of *Rb. sphaeroides* as described by Paddock et al. (1989). Several exconjugants were picked and checked for the plasmid. To confirm that the desired mutation in the puf M gene was introduced into *Rb. sphaeroides*, the pRKNEB1 plasmid bearing the mutation was isolated from *Rb. sphaeroides* and the BamHI-Sall fragment was sequenced after being cloned again in M13 bacteriophage.

Chromatophores were obtained from a sonicated cell suspension. Sonication was performed with a 300 W sonifier for 10 min at 4°C. Isolated chromatophores were resuspended in 100 mM phosphate buffer, pH 7.5. The RCs were extracted with 0.25% LDAO by two consecutive incubations (45 min and 30 min) of chromatophores resuspended to a concentration of $OD_{865} = 30/\text{cm}$. After the second incubation, the RCs were precipitated with 26% ammonium sulfate, resuspended in 10 mM Tris-HCl pH 8

containing 0.1% LDAO and desalted using a sephadex G-50 column. The solution was then loaded at room temperature on a Q-sepharose column which was washed with 10 mM Tris-HCl pH 8 containing 0.1% LDAO (TL buffer), after which the RCs were eluted using a 100–600 mM NaCl gradient. This purification procedure was necessary in order to separate the RCs from a minor contamination with light-harvesting complex that sometimes was extracted together with the RCs. After dialysis against TL buffer, the RCs were passed through a DEAE sephacel column at 4°C, washed, and eluted with a 100–300 mM NaCl gradient. The RCs were then dialyzed against TL buffer and concentrated over a 100 kD Amicon filter. The A_{280}/A_{802} and A_{280}/A_{806} ratios for the wild type and the mutant, were between 1.2 and 1.4, respectively. Throughout this work 'wild type' refers to the deletion mutant complemented with wild-type genes.

Absorption, fluorescence emission and fluorescence excitation spectroscopy were performed using a single-beam spectrophotometer, equipped with a personal computer for data analysis as described by Otte et al. (1991). The spectral resolution was 0.5 nm and 3.0 nm for absorption and fluorescence measurements, respectively. The intensity of the excitation light was less than $50 \mu\text{W}/\text{cm}^2$. Glycerol (60% v/v) was added to all samples used in low-temperature experiments. The final absorbance was always less than 0.2 OD at the peak of the accessory BChl absorption band (802 nm for the wild type and 806 nm for the mutant).

The transient absorption data were obtained with a sub-picosecond laser system operating at 50 Hz (Dressler et al. 1991, Schmidt et al. 1993). The sample was held in a 1 mm cuvette with an optical density of about 0.5 at 870 nm. Excitation was at 870 nm; about 10% of the RCs were excited per laser pulse. Stirring of the sample prevented accumulation of oxidized P in the excitation beam. The width of the instrumental response function was around 300 fs. For measurements on a slower time scale, a ps spectrophotometer was used with a pulse width of 30 ps as described (Schelvis et al. 1992); optical changes on a ms time scale were measured with an absorption-difference spectrophotometer de-

scribed by Visser (1975). All optical experiments were performed at room temperature. EPR measurements were carried out at about 120 K with an X-band Varian E-9 spectrometer as described by Gast and Hoff (1979).

The ADMR (Absorbance-Detected Magnetic Resonance) and LD-ADMR (Linear-Dichroic ADMR) set-ups are described in detail by Den Blanken et al. (1984). A single tungsten-iodine lamp is used for continuous excitation and as the source of the detection beam. Amplitude modulation of the microwaves and subsequent phase-sensitive detection of the resulting modulation in transmittance results in a Triplet-minus-Singlet ($T-S$) absorbance spectrum. The optical density of RCs used in these experiments was about 0.3 at 802 nm. For reducing the primary electron acceptor Q_A , 10 mM sodium ascorbate was added, and the sample was frozen under illumination with white light. Glycerol (66% V/V) was added to obtain a clear sample. The ADMR and (LD)-ADMR measurements were carried out at 1.2 K.

Results

Growth characteristics

The mutant (M)Y210W was capable of photoheterotrophic growth tested at a light intensity of 50 W/m^2 . This was determined by comparing the number of colonies on plates at several dilutions (starting from the same inoculum of cells grown semi-aerobically) under photoheterotrophic and chemoheterotrophic conditions. We found the same number of colonies under both conditions.

The RCs are photochemically active as demonstrated by the reversible bleaching of the long-wavelength absorption band of P by actinic light (data not shown). The amplitude of the photobleaching at 865 nm in a suspension of chromatophores of mutant or wild type, containing equal concentration of bacteriochlorophyll, was the same for both. This indicates that the amount of RCs in the photosynthetic membranes of the (M)Y210W mutant is comparable to that of the wild type.

By monitoring the kinetics of the reversible photobleaching at 865 nm on a ms-time scale

(data not shown), it was found that for mutant RCs at least 90% of the Q_A sites and 60% of the Q_B sites were occupied after the isolation procedure. In the wild type RC virtually all Q_A and Q_B were still present.

Low-temperature steady-state spectroscopy

The absorption spectra of isolated RCs of the wild type and the (M)Y210W mutant are shown in Figs. 1A and 1B, respectively. Whereas some differences are detected at room temperature (dashed lines), they become more apparent at 6 K (solid lines). At this low temperature the Q_y band of the accessory BChl is shifted to 806 nm for the mutant, compared to 802 nm for the wild type. The bacteriopheophytin Q_y band showed a blue shift of 4 nm to 757 nm. The exact position of the Q_y band of the primary electron donor P depended on sample preparation and varied from 896 nm to 900 nm. This band was always found at 896 nm in RCs isolated from the wild

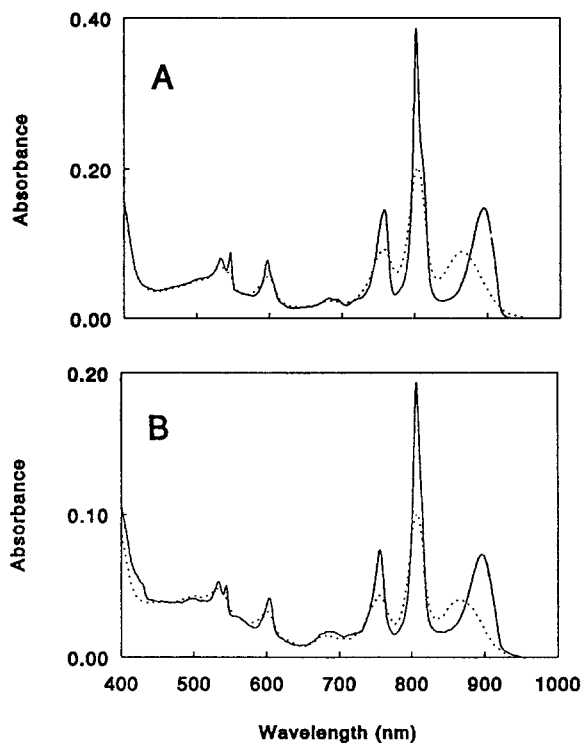


Fig. 1. Absorption spectra of isolated RCs of wild type (A) and the (M)Y210W mutant (B) at room temperature (dashed lines) and 6 K (solid lines). See 'Materials and methods' for the experimental conditions.

type. In the Q_x region the wild type has a band at 597 nm, with a shoulder at 606 nm, as revealed by the second derivative spectrum (not shown). The 597 nm band was attributed to the Q_x transition of the 800 nm BChl. The 606 nm band was suggested to represent at least partly the Q_x band of P, with possibly a contribution of the Q_x band of B_B (Kirmaier et al. 1985). Similar to the mutants discussed by Gray et al. (1990) and Mattioli et al. (1990), the 597 nm band of the wild type exhibits a red shift to 604 nm in the mutant; consequently it then overlaps with the component at 606 nm. The absorption band of Φ_A for the wild type was located at 547 nm; for the mutant this band was blue shifted 2 nm to 545 nm. The absorption band of Φ_B at 535 nm is virtually unaffected by the tryptophan substitution.

The fluorescence emission spectra at 6 K of open RCs of the mutant and the wild type are given in Fig. 2 for excitation at the BChl Q_x band. The mutant showed a pronounced emis-

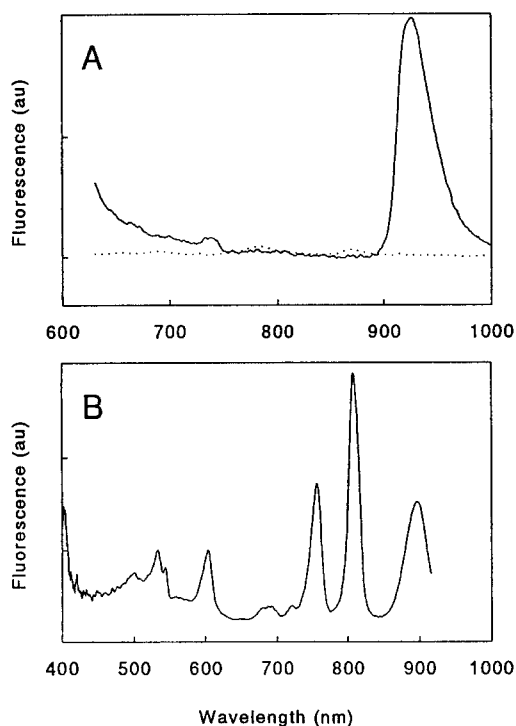


Fig. 2. (A) Fluorescence emission spectra of RCs of the wild type (dashed line) and the (M)Y210W mutant (solid line) at 6 K with excitation given at 597 and 603 nm, respectively. (B) Fluorescence excitation spectrum of mutant RCs at 6 K; the detection wavelength was 930 nm.

sion band at 926 nm (Fig. 2A), which we attribute to fluorescence from the excited singlet state of P, P^* . No fluorescence band at that wavelength was observed for the wild-type RCs, both at 6 K (Fig. 2A) and at room temperature (data not shown). The yield of the fluorescence was estimated using a suspension of chromatophores of *Rhodospirillum rubrum* as a standard, assuming a 1–5% fluorescence yield for the chromatophores (Wang and Clayton 1971). The yield of the 926 nm emission band for the mutant was 0.1–0.6% at 6 K, and four times lower at 298 K. The yield at 6 K for the wild type was at least 20 times lower than that for the mutant.

The fluorescence excitation spectrum of the mutant at 6 K (Fig. 2B) is very similar to the low-temperature absorption spectrum, indicating that all RC pigments transfer the excitation energy efficiently to P (Breton et al. 1986).

The EPR linewidth (ΔH_{pp}) of P^+ was 9.7 ± 0.2 G for both mutant and wild-type RCs.

Primary charge separation

The dynamics of the primary charge separation was studied by probing the lifetime of the excited electronic state P^* at room temperature at 920 nm. Figure 3 shows the transient absorption curves of the wild type (Fig. 3A) and the (M)Y210W mutant (Fig. 3B) RC. The absorbance decrease at 920 nm at early delay times is due to stimulated emission from the excited electronic level of P^* . Its decay rate reflects the depopulation of the excited primary donor. It is, therefore, to first approximation identical to the rate of charge separation.

The decay of P^* in the wild type was fitted to an exponential function with a time constant of 2.8 ps. The systematic deviation between fit and data points in the 10 ps regime may be reduced using two time constants (e.g. 2.3 ps and 7 ps as found in Hamm et al. (1993)). The late relative absorbance decrease can be fitted with a 220 ps time constant. This time constant is due to the electron transfer from Φ_A to Q_A (Holzapfel et al. 1990). The decay of P^* in the (M)Y210W mutant was best fitted by a sum of two exponentials with time constants of 5.1 ± 0.8 ps (20%) and 36.0 ± 1.8 ps (70%). The residual amplitudes (6% in the wild type and 10% in the mutant), are due to

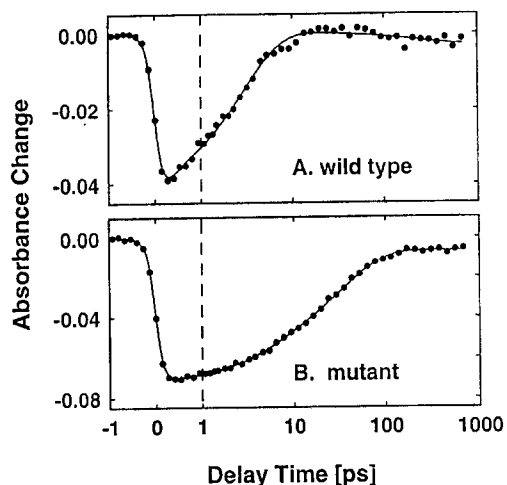


Fig. 3. Transient absorption kinetics of RCs isolated from the wild type (A) and the (M)Y210W mutant (B), measured at a probing wavelength of 920 nm. The absorbance change in the wild type was fitted with a sum of two exponentials having a time constant of 2.8 ps and 220 ps. The kinetics in the (M)Y210W mutant was best fitted with two exponentials with a time constant of 5.1 ± 0.8 ps and 36.0 ± 1.8 ps. The residual amplitudes at late delay times is due to $P^+Q_A^-$. At early delay times ($t < 1$ ps), a linear timescale and, for later times ($t > 1$ ps), a logarithmic scale is used.

$P^+Q_A^-$ absorption (Van Noort et al., manuscript in preparation).

ADMR and LD-ADMR

ADMR spectroscopy of the mutant RC at a detection wavelength of 905 nm (the peak of the long-wavelength absorption band at 1.2 K) yielded two zero-field (zf) transitions of the primary donor triplet, P^T (data not shown). The maximum of the $|D| - |E|$ transition was at 463 MHz; that of the $|D| + |E|$ transition at 656 MHz, where D and E represent the zero-field splitting (ZFS) parameters. For different detection wavelengths within the long-wavelength band (centered at 905 nm), the zero-field frequencies shift with the detection wavelength, similar to the behavior found for RCs of *Rb. sphaeroides* R26 (Den Blanken et al. 1983) and RCs of other purple bacteria (J. Vrieze, unpublished results). This shift has been attributed to heterogeneity with respect to the exact configuration of the primary donor (Den Blanken et al. 1983). At the absorption peak of the T-S spectrum, which is attributed to accessory bacteriochlorophyll

(Scherer and Fischer 1987) and located at 808 nm for the wild type and 809 nm for the mutant, the shift of the zero-field frequencies with detection wavelength is very small. The ZFS parameters determined at this wavelength are $|D| = 189.5 \pm 0.3 \cdot 10^{-4} \text{ cm}^{-1}$ and $|E| = 32.2 \pm 0.2 \cdot 10^{-4} \text{ cm}^{-1}$ (Fig. 4). These values are virtually the same as found for wild-type RCs at the corresponding wavelength of 808 nm ($|D| = 187.3 \cdot 10^{-4} \text{ cm}^{-1}$ and $|E| = 31.7 \cdot 10^{-4} \text{ cm}^{-1}$). The decay rates of the three triplet sublevels are also practically identical to those measured for the wild-type RCs (data not shown). Thus, the properties of the triplet state of the primary donor do not change on introducing the (M)Y210W mutation.

T-S and LD(T-S) spectra of wild-type and mutant RCs are shown in Fig. 5. The T-S and LD(T-S) spectra were measured at 463 and 656 MHz. Some differences are observed between the T-S spectra of the mutant and the wild type. The positive 809 nm band of the mutant is lower in intensity than the corresponding band of the wild type and redshifted by 1 nm, most probably because of a shift in the $S_1 \leftarrow S_0$ transition in the absorption spectrum from 802 to 806 nm, which leads to a stronger overlap of the 808 nm band with the adjacent negative band in the T-S spectrum. The intensity of the 820 nm band is equal for the wild type and the mutant, which is in agreement with the identical peak wavelength and intensity of the 814 nm band in the deconvoluted $S_1 \leftarrow S_0$ absorption spectrum of the two species. The low-energy band of the primary donor of the

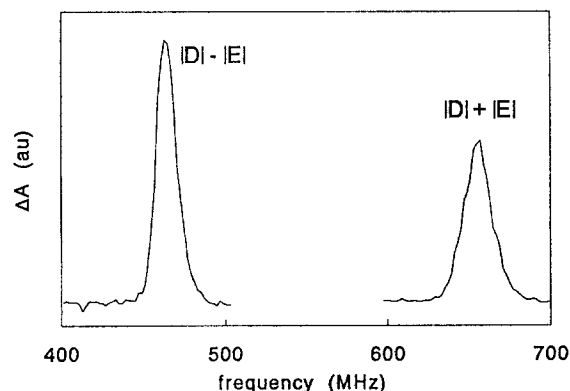


Fig. 4. ADMR-detected zero-field transitions of the mutant RC at 1.2 K. The detection wavelength was 809 nm.

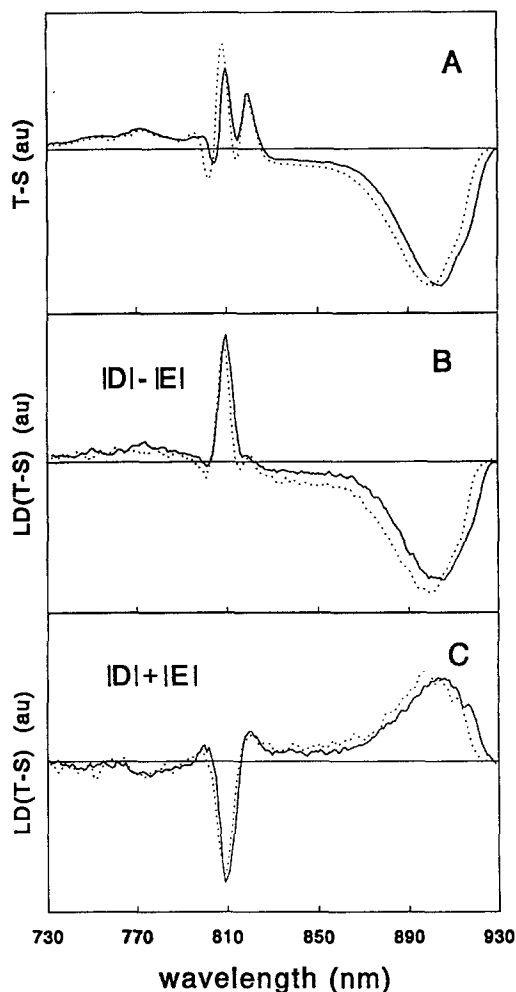


Fig. 5. (A) (T-S) spectra monitored at 463 MHz, (B) LD (T-S) spectra monitored at 463 MHz, (C) LD (T-S) spectra monitored at 656 MHz. for wild-type (dotted line) and mutant (solid line) RCs.

mutant has red-shifted by 4 nm compared to that of the wild type, both in the T-S and in the absorption spectrum, measured under the same conditions.

The LD(T-S) spectrum represents the difference between the T-S spectrum measured with the polarization of the probe beam parallel and perpendicular to the magnetic field vector of the microwave field. The angle α_i between the optical transition moment μ° of a given absorption band in the T-S spectrum and the triplet spin axis i can be determined from the ratio R_i between the amplitude of the T-S and the LD(T-S) signal at that wavelength, using (Hoff et al. 1985):

$$R_i = \frac{\text{LD(T-S)}}{\text{T-S}} = \frac{3 \cos^2 \alpha_i - 1}{\cos^2 \alpha_i + 3}$$

The microwave power must be low enough to fulfill the condition of a truly random sample. Experimentally, this condition is met by measuring R_i as a function of microwave power and extrapolating to the zero-power limit. In RCs the experimentally accessible spin axes are the y- and x-axes, corresponding to the $|D| - |E|$ and the $|D| + |E|$ transition of P^T , respectively, where we take $D > 0$ and $E > 0$ as in Thurnauer and Norris (1977). Measurement of R_i for two directions i (two zero-field transitions) fixes the optical transition moment in the (x, y, z) microwave coordinate frame, to a fourfold degeneracy. Using the $|D| - |E|$ and the $|D| + |E|$ transitions of the mutant, we found for the 905 nm band $R_y = 0.43$ and $R_x = 0.28$, yielding $\alpha_y = 24^\circ \pm 2^\circ$ and $\alpha_x = 80^\circ \pm 5^\circ$. For the wild type the angles were: $\alpha_y = 20^\circ \pm 2^\circ$ and $\alpha_x = 85^\circ \pm 5^\circ$.

The shapes of the LD(T-S) spectra of the mutant and the wild type in the 790–820 nm region are essentially the same. From this, and from the difference in shape of the two T-S spectra, we can immediately conclude that the R-value(s), defined by Eq. (1), have changed for one or more absorption bands in the 790–820 nm region of the T-S spectrum. Comparing the T-S and the LD(T-S) spectra, the change in the ratio $R_{x,y}$, measured at 808 nm, could result from a change in the direction of the 808 nm optical transition moment, such that it is more parallel to the triplet y-axis and thus more perpendicular to the triplet x-axis in the mutant compared to the wild type. Because positive and negative bands are strongly overlapping in the 790–820 nm region of the T-S spectrum, however, this change in LD(T-S)/T-S value at 808 nm can also be explained by a smaller absolute R value of the adjacent negative 806 nm and/or 814 nm bands.

Discussion

Absorption spectra

The absorption spectrum (Fig. 1) shows that several bands have shifted because of the muta-

tion. This is best seen in the spectrum at 6 K, where the bands are narrowed (Fig. 1B). Differences were found in the Q_y and Q_x regions of BChl, as has been observed for other mutants (Gray et al. 1990, Mattioli et al. 1991). The BChl Q_x region of the absorption spectrum, with contributions of B_A , B_B and P, shows a close similarity with the 800 nm region. On mutation, only the 802 nm BChl band, which was attributed to B_A (Kirmaier et al. 1985), exhibited a red shift, whereas the energy levels of B_B and P remained unchanged. Assuming that the band shift in the Q_x region correlates with that of the Q_y region, we assign the red-shifting 597 nm band to B_A , and the unchanged 606 nm shoulder to P. A blue shift of 2 nm observed at the 547 nm band, attributed to Φ_A , corresponded with the blue shift in the Q_y region. The low-energy band of P at low temperature does not shift, suggesting that the mutation has no effect on the special pair. This is corroborated by the $|D|$ and $|E|$ values of the triplet, obtained by ADMR measurements and by the value of the EPR linewidth of P^+ (9.7 G), which are the same for the wild type and the mutant.

Fluorescence spectra and yields

The low-temperature fluorescence spectra show efficient energy transfer from the chromophores to P (Fig. 2B). The strong fluorescence emission band at 926 nm could be due to a slower charge separation rate at 6 K. Assuming that the steady state fluorescence emission is not due to inactive RCs (with longer lifetime of P^*), one can draw conclusions on the temperature dependence of the electron transfer. The relative fluorescence yield of the mutant RC was four times lower at room temperature than at 6 K, while the yield of the wild type RC was at 6 K at least 20 times lower than that of the mutant RC. For a temperature-independent fluorescence yield of the wild type (Woodbury and Parson 1984), the ratio of the fluorescence yield for mutant/wild type at room temperature is larger than 5. This estimate compares reasonably well with the strong increase in the lifetime of P^* going from the wild type to the mutant RCs. The four times higher fluorescence yield in the mutant at 6 K compared to room temperature, predicts that the lifetime

of P^* increases to more than 100 ps at 6 K, making charge separation at least 50 times slower than that of the wild type at this temperature. This strong temperature dependence supports the idea that the electron transfer in the mutant is thermally activated at room temperature and that the reaction mechanism may change at low temperature, e.g. from a stepwise electron transfer to a superexchange mechanism.

Structural changes

Since tryptophan is a rather large residue, it could cause a structural change in the protein, which could influence the charge-separation rate in unpredictable ways. The measurements performed with ADMR spectroscopy give us some information on these structural changes, if any.

The ZFS-parameters and the decay rates of the sublevels of the primary donor triplet depend on the structure and the environment of P. Both observables have virtually the same values for the mutant and the wild type, indicating that on mutation there are no changes in the structure and the environment of the primary donor that influences its properties in the triplet state. A small difference in the $LD(T-S)/(T-S)$ ratio for the mutant and the wild type might implicate that the angles between the optical transition moments contributing to the 790–820 nm region and the triplet axes have been altered slightly by the mutation (Fig. 4). The 802 nm band has been attributed mainly to B_A with some contribution from Φ_A and the 814 nm band mainly to B_B , possibly with some contribution from the high-energy exciton component of P (Kirmaier et al. 1985). With this assignment, the shift of the 802 nm band (wild type) to longer wavelength (806 nm) and the blue shift of the Φ_A band can be attributed to a stronger exciton coupling between B_A and Φ_A . Upon triplet formation both the 806 nm band and the 814 nm shift to shorter wavelength, the 806 nm band to about 800 nm and the 814 nm band to 808 nm. The 808 nm band appearing upon triplet formation is therefore attributed to B_B and is not affected by the mutation. With this interpretation, it is unlikely that the apparent change in R-value observed at 808 nm band is caused by a change in R-value of the 808 nm band. It seems more

probable that the adjacent negative 806 nm band gives rise to the observed changes in R-value. The change in R-value of the 806 nm band should correspond to its transition moment becoming less parallel to the donor triplet y-axis. Since the optical transition moment of P (900 nm) is almost parallel to this triplet y-axis, the optical transition moment of the B_A (the main contributor to the 806 nm band) also becomes less parallel to the optical transition moment of P in the mutant compared to the wild type.

Summarizing, the absorption and the T-S spectra could be simulated by an increase of the (B_A , Φ_A) interaction. Furthermore, a less parallel alignment of the transition moment of B_A and P will decrease the interaction of (P, B_A) without changing other parameters, such as zero-order energies and dipole strengths.

The change in the (B_A , Φ_A) interaction can be explained by a difference in orientation or position of B_A or Φ_A . A displacement of B_A towards Φ_A or vice versa will increase the (B_A , Φ_A) interaction. A rotation of the Q_Y transition of the B_A moment towards the C_2 -symmetry axis has the same effect. In the simple exciton model used, the influence of changes in the environment (amino acids) on the energies and the dipole strengths of the chromophores are not taken into account. Although such an indirect effect on the dipolar strength of B_A or Φ_A cannot be excluded, preliminary CP-MAS NMR results (Shochat et al., manuscript in preparation) indicate that no major changes occur in the ^{13}C -labeled Tyr signals of the mutant.

Using molecular orbital calculations, Plato et al. (1988) explained the unidirectionality partially by an orbital overlap between P and B_A that is stronger than that between P and B_B . In our description, the orbital overlap between P and B_A will be smaller for the mutant compared to the wild type, both for a displacement of B_A towards Φ_A , and a rotation of its Q_Y transition moment towards the C_2 -symmetry axis. In the latter case, the optical Q_Y transition moments of P and B_A and, therefore, the macrocycle planes, are less parallel for the mutant than for the wild type. The resulting decrease of orbital overlap of P and B_A might lower the rate of charge separation in the L-chain.

Charge-separation kinetics

The replacement of tyrosine (M)Y210 by a tryptophan affects the initial electron transfer step significantly. Room-temperature sub-picosecond spectroscopy shows that the decay of P^* is bi-exponential, with a main, slow time constant of 36 ps and a weak, additional, fast time constant of 5.1 ps (Fig. 3). Similar time constants were observed at 660 nm, which is the probing wavelength for the formation of the charge-separated $P^+\Phi_A^-$ state (data not shown). Comparing the charge-separation rates with those of previously reported, analogous mutants (Gray et al. 1990, Nagarajan et al. 1990, Chan et al. 1991, Hamm et al. 1993), the (M)Y210W mutant appears to have the slowest charge-separation rate component of all reported mutants to date. A similar result (a time constant of 35 ± 3 ps) was reported by Nagarajan et al. (1992) for the same mutation. This component is more than ten times slower than in the wild type (assuming a single exponential decay). Nagarajan et al. (1992) found a qualitative correlation between the increase in the midpoint redox potential for the oxidation of P and the slow-down of the electron transfer in several mutants including the (M)Y210W mutant. It is possible that the slow charge-separation rate results from two effects, a change in redox potential of P (caused, for example, by the different polarizability and local charge density of the tryptophan, Parson et al. (1990)) and the decrease in orbital overlap of P and B_A , suggested by the ADMR measurements. Alternatively, the replacement of tyrosine (M)Y210 by tryptophan could alter the energy level of the intermediate state $P^+B_B^-$ (see for example Parson et al. (1990)), and thereby slow down the charge-separation rate. This could also lead to the involvement of a parking state $P^+B_B^-$.

Bi-exponential kinetics of the time-resolved absorption have been found at 920 nm for *Rb. sphaeroides* and *Rb. capsulatus* mutants in which tyrosine-(M)210 had been exchanged by phenylalanine (Finkele et al. 1990, Chan et al. 1991, Hamm et al. 1993), and leucine (Finkele et al. 1990). But for most mutations on the tyrosine-(M)210 site, the kinetics at room temperature were fitted with single exponentials (Nagarajan et al. 1990, Chan et al. 1991). Recent studies on

femtosecond spontaneous- and stimulated-emission studies have shown that for all RCs studied (*Rb. sphaeroides* R-26, (Du et al. 1992); (M)Y210P, (L)P181Y and the corresponding double mutant (Hamm et al. 1993), *Chloroflexus aurantiacus* (Martin et al. 1990, Feick et al. 1990, Becker et al. 1991, Müller et al. 1992, Hamm et al. 1992, Hamm et al. 1993) and *Rb. capsulatus* wild type, (M)Y210P, (L)P181Y and the corresponding double mutant (Du et al. 1992)), the kinetics of the decay of the spontaneous emission of P^* are bi-modal.

Nagarajan et al. (1990) explained the non-exponential reaction kinetics in terms of a conformational heterogeneity in the sample, induced by a lack of stabilizing influence of the rigid aromatic ring or the phenolic group upon mutation. They suggested that this effect might be more evident at low temperatures where inter-conversion among different conformational states would occur relatively slowly. Since tryptophan is a relatively bulky residue, it is hard to conceive two different conformations of the protein that could easily interconvert. Moreover, ^{13}C MAS-NMR spectra of RCs of the (M)Y210W mutant do not suggest the existence of two distinctly different conformations (S. Shochat et al., manuscript in preparation). Therefore, this kind of two-state heterogeneity does not seem to apply in our case. It is not excluded, however, that more subtle heterogeneities, leading to a distribution of many slightly different states, are the cause of the apparent biphasic kinetics. Kirmayer and Holten (1990) suggested a distribution of RCs with different rates of electron transfer. If the different RCs in the distribution interconvert on a time scale longer than that of the primary photochemistry, then this would lead to non-exponential kinetics of the primary electron transfer. As a possible cause for such an inhomogeneous distribution, differences in the degree of hydrogen bonding between the C-10 keto group of Φ_A and the adjacent glutamic acid residue (Glu L104) were cited. Based on spontaneous emission studies, Norris and Fleming (personal communication) also suggested that a distribution of conformations could lead to an apparent biphasic decay pattern of the emission. Computer simulations (R. van der Vos, unpublished results)

indicate that a Gaussian distribution of the difference in free energy ΔG between the initial and the product states, which is related to the charge separation by the Marcus equation (Marcus 1956), indeed may result in a decay pattern that can be fitted with a bi-exponential function, within the signal-to-noise ratio of the ps-measurements. Evidence for heterogeneity of P conformation was also reported by Den Blanken et al. (1983), who observed in ADMR experiments a pronounced dependence of the primary donor bleaching in the triplet-singlet difference spectrum on the applied microwave field. A contrasting view was advanced by Lyle et al. (1993), who on the basis of hole-burning studies proposed that the role inhomogeneities involving the structure or energetics of P, play in the charge-separation kinetic, is limited.

Finally, the biphasic decay of P^* could be explained by assuming that an additional intermediate, a so-called parking state, is involved. Time-resolved fluorescence experiments showing bi-exponential decay of the excited primary donor in wild type RCs of *Rb. sphaeroides*, suggested to Müller et al. (1992) and Hamm et al. (1993) that such a state could involve chromophores on the inactive B-branch. Temporarily parking the excitation energy of the excited primary donor in the inactive B-branch by either energy transfer, or by formation of a real charge-separated state $P^+B_B^-$ or $P^+\Phi_B^-$, results in bi-exponential decay of the excited primary donor.

Conclusions

We have shown that the charge-separation process in the RC of the (M)Y210W mutant of *Rb. sphaeroides* showed bi-exponential kinetics at room temperature with a main time constant of 36 ps and an additional fast time constant of 5.1 ps. The fluorescence yield of these RCs was four times higher at 6 K than at room temperature. This could be due to an increase in the lifetime of P^* at cryogenic temperatures. EPR and ADMR measurements indicate that the dimeric structure of P is not altered significantly by the mutation. In contrast, the interaction of the accessory bacteriochlorophyll B_A with its environment appears to be altered in the mutant,

possibly because of a change in its position. This could be one of the factors that causes the slower charge-separation rate in the mutant.

Acknowledgments

This work was supported by The Netherlands Foundations for Chemical Research (SON) and for Biophysics, financed by The Netherlands Organization for Scientific Research (NWO) and by Twinning Grant No SC 1-CT90-0569 of the European Community. P.G. is a research fellow of the Royal Netherlands Academy of Arts and Sciences. We are grateful to Jan Schutrups and Saskia Jansen for their help with RC preparations and to H.J.M. de Groot for helpful discussions. S.S. thanks Prof L. Bosch and other members of the Department of Biochemistry, Leiden University, for their hospitality.

References

- Allen JP, Feher G, Yeates TO, Komiya H and Rees DC (1987a) Structure of the reaction center from *Rhodobacter sphaeroides* R-26: The cofactors. *Proc Natl Acad Sci USA* 84: 5730-5734
- Allen JP, Feher G, Yeates TO, Komiya H and Rees DC (1987b) Structure of the reaction center from *Rhodobacter sphaeroides* R-26: The protein subunits. *Proc Natl Acad Sci USA* 84: 6162-6166
- Becker M, Nagarajan V, Middendorf D, Parson WW, Martin JE and Blankenship RE (1991) Temperature dependence of the initial electron-transfer kinetics in photosynthetic reaction centers of *Chloroflexus aurantiacus*. *Biochim Biophys Acta* 1057: 299-312
- Breton J, Martin JL, Migus A, Antonetti A and Orszag A (1986) Femtosecond spectroscopy of excitation energy transfer and initial charge separation in the reaction center of the photosynthetic bacterium *Rhodospseudomonas viridis*. *Proc Natl Acad Sci USA* 83: 5121-5125
- Chan CK, Chen LXQ, DiMugno TJ, Hanson DK, Nance SL, Schiffer M, Norris JR and Fleming GR (1991) Initial electron transfer in photosynthetic reaction centers of *Rhodobacter capsulatus* mutants. *Chem Phys Lett* 176: 366-372
- Den Blanken HJ and Hoff AJ (1983) Resolution enhancement of the triplet-singlet absorbance difference spectrum and the triplet-ESR spectrum in zero field by the selection of sites. An application to photosynthetic reaction centers. *Chem Phys Lett* 98: 255-261
- Den Blanken HJ, Meiburg RF and Hoff AJ (1984) Polarized triplet-minus-singlet absorbance difference spectra measured by absorbance-detected magnetic resonance. An application to photosynthetic reaction centres. *Chem Phys Lett* 105: 336-342
- Dressler K, Umlauf E, Schmidt S, Hamm P, Zinth W, Buchanan S and Michel H (1991) Detailed studies of the subpicosecond kinetics in the primary electron transfer of reaction centers of *Rhodospseudomonas viridis*. *Chem Phys Lett* 183: 270-276
- Du M, Rosenthal SJ, Xie X, DiMugno TJ, Schmidt M, Hanson DK, Schiffer M, Norris JR and Fleming GR (1992) Femtosecond spontaneous-emission studies of reaction centers from photosynthetic bacteria. *Proc Natl Acad Sci USA* 89: 8517-8521
- Feick R, Martin JL, Breton J, Volk M, Scheidel G, Langenbacher T, Urbano C, Ogrognik A and Michel-Beyerle ME (1990) Biexponential charge separation and monoexponential decay of $P^+ H^-$ in reaction centers of *Chloroflexus aurantiacus*. In: Michel-Beyerle ME (ed) *Reaction Centers of Photosynthetic Bacteria*, pp 181-188, Springer Series in Biophysics Vol 6. Springer-Verlag, Heidelberg
- Finkele U, Lauterwasser C, Zinth W, Gray KA and Oesterhelt D (1990) Role of tyrosine M210 in the initial charge separation of reaction centers of *Rhodobacter sphaeroides*. *Biochemistry* 29: 8517-8521
- Fischer MR, De Groot HJM, Raap J, Winkel C, Hoff AJ and Lugtenburg J (1992) ^{13}C magic angle spinning NMR study of the light-induced and temperature-dependent changes in *Rhodobacter sphaeroides* R26 reaction centers enriched in [$4'-^{13}C$] tyrosine. *Biochemistry* 31: 11038-11049
- Gast P and Hoff AJ (1979) Transfer of light-induced electron-spin polarization from the intermediate acceptor to the prerduced primary acceptor in the reaction center of photosynthetic bacteria. *Biochim Biophys Acta* 548: 520-535
- Gray KA, Farchaus JW, Wachtveitl J, Breton J and Oesterhelt D (1990) Initial characterization of site-directed mutants of tyrosine M210 in the reaction center of *Rhodobacter sphaeroides*. *EMBO J* 9: 2061-2070
- Hamm P, Gray KA, Oesterhelt D, Feick R, Scheer H and Zinth W (1993) Subpicosecond emission studies of bacterial reaction centers. *Biochim Biophys Acta* 1142: 99-105
- Hoff AJ (1982) ODMR Spectroscopy in Photosynthesis II. The Reaction Center Triplet in Bacterial Photosynthesis. In: Clark RH (ed) *Triplet State ODMR Spectroscopy*, pp 367-425. John Wiley & Sons, New York
- Hoff AJ, den Blanken HJ, Vasmel H and Meiburg RF (1985) Linear-dichroic triplet-minus-singlet absorbance difference spectra of reaction centers of the photosynthetic bacteria *Chromatium vinosum*, *Rhodospseudomonas sphaeroides* R-26 and *Rhodospirillum rubrum*. *Biochim Biophys Acta* 806: 389-397
- Holzappel W, Finkele U, Kaiser W, Oesterhelt D, Scheer H, Stiltz HU and Zinth W (1990) Initial electron-transfer in the reaction center from *Rhodobacter sphaeroides*. *Proc Natl Acad Sci USA* 87: 5168-5172
- Kirmaier C and Holten D (1987) Primary photochemistry of reaction centers from the photosynthetic purple bacteria. *Photosynth Res* 13: 225-260
- Kirmaier C, Holten D and Parson WW (1985) Picosecond-photodichroism studies of the transient states in *Rhodospseudomonas sphaeroides* reaction centers at 5 K. Effects

- of electron transfer on the six bacteriochlorin pigments. *Biochim Biophys Acta* 810: 49–61
- Kunkel TA (1987) Rapid and efficient site-specific mutagenesis without phenotypic selection. *Proc Natl Acad Sci USA* 82: 488–492
- Lyle PA, Kolaczowski SV and Small GJ (1993) Photochemical hole-burning spectra of protonated and deuterated reaction centers of *Rhodobacter sphaeroides*. *J Phys Chem* 97: 6924–6933
- Marcus RA (1956) On the theory of oxidation-reduction reactions involving electron transfer. I. *J Chem Phys* 24: 966–978
- Martin JL, Lambry JC, Ashokkumar M, Michel-Beyerle ME, Feick R and Breton J (1990) Primary charge separation in reaction centers of *Chloroflexus aurantiacus* bacterium. In: Harris CB, Ippen EP, Mourruo GA and Zewail AH (eds) *Ultrafast Phenomena VII*, pp 524–528. Springer Series in Chemical Physics, Vol 53. Springer-Verlag, Heidelberg
- Mattioli TA, Gray KA, Lutz M, Oesterhelt D and Robert B (1991) Resonance Raman Characterization of *Rhodobacter sphaeroides* reaction centers bearing site-directed mutations at tyrosine M210. *Biochemistry* 30: 1715–1722
- Michel H, Epp O and Deisenhofer J (1986) Pigment-protein interactions in the photosynthetic reaction centre from *Rhodospirillum rubrum*. *EMBO J* 5: 2445–2451
- Müller MG, Griebenow K and Holzwarth AR (1992) Primary processes in isolated bacterial reaction centers from *Rhodobacter-sphaeroides* studied by picosecond fluorescence kinetics. *Chem Phys Lett* 199: 465–469
- Nagarajan V, Parson WW, Gaul D and Schenck C (1990) Effect of specific mutations of tyrosine-(M)210 on the primary photosynthetic electron-transfer process in *Rhodobacter sphaeroides*. *Proc Natl Acad Sci USA* 87: 7888–7892
- Nagarajan V, Davis D, Parson W and Schenck C (1992) Abstracts of the Cadarache NATO Workshop on 'Structure, Function and Dynamics of the Bacterial Reaction Center', May 10–15
- Otte SCM, Vanderheiden JC, Pfennig N and Ames J (1991) A comparative study of the optical characteristics of intact cells of photosynthetic green sulfur bacteria containing bacteriochlorophyll *c*, *d* or *e*. *Photosynth Res* 28: 77–87
- Paddock ML, Rongey SH, Feher G and Okamura MY (1989) Pathway of proton transfer in bacterial reaction centers: Replacement of glutamic acid 212 in the L subunit by glutamine inhibits quinone (secondary acceptor) turnover. *Proc Natl Acad Sci USA* 86: 6602–6606
- Parson WW, Chu Z-T and Warshel A (1990) Electrostatic control of charge separation in bacterial photosynthesis. *Biochim Biophys Acta* 1017: 251–272
- Plato M, Mobius K, Michel-Beyerle ME, Bixon M and Jortner J (1988) Intermolecular electronic interactions in the primary charge separation in bacterial photosynthesis. *J Am Chem Soc* 110: 7279–7285
- Schelvis JPM, Liu BL, Aartsma TJ and Hoff AJ (1992) The electron transfer rate from BPh_A to Q_A in reaction centers of *Rhodobacter sphaeroides* R-26 – Influence of the H-subunit, the Q_A and Fe-2 + cofactors, and the isoprene tail of Q_A. *Biochim Biophys Acta* 1102: 229–236
- Scherer POJ and Fischer SF (1987) Model studies to low-temperature optical transitions of photosynthetic reaction centers. II. *Rhodobacter sphaeroides* and *Chloroflexus aurantiacus*. *Biochim Biophys Acta* 891: 157–164
- Schmidt S, Arlt T, Hamm P, Lauterwasser C, Finkele U, Drews G and Zinth W (1993) Time-resolved spectroscopy of the primary photosynthetic processes of membrane-bound reaction centers from an antenna-deficient mutant of *Rhodobacter capsulatus*. *Biochim Biophys Acta* 1144: 385–390
- Shiozawa JA, Lottspeich F, Oesterhelt D and Feick R (1989) The primary structure of the *Chloroflexus aurantiacus* reaction-center polypeptides. *Eur J Biochem* 180: 75–84
- Shochat S, Van Noort PI, Van der Vos R, Otte SCM, Schelvis H, Vrieze J, Kleinherenbrink FAM, Gast P and Hoff AJ (1992) Spectroscopic characterization of reaction centers of the M^{Tyr 210} → ^{Trp} mutant of *Rhodobacter sphaeroides*. In: Murata N (ed) *Proceedings of the IXth International Congress on Photosynthesis*, pp 413–416. Kluwer Academic Publishers, Dordrecht
- Thurnauer MC and Norris JR (1977) The ordering of the zero field triplet spin sublevels in the chlorophylls. A magnetophotoselection study. *Chem Phys Lett* 47: 100–112
- Visser JWM (1975) Photosynthetic reactions at low temperatures. PhD thesis, Leiden University
- Wang RT and Clayton RK (1971) The absolute yield of bacteriochlorophyll fluorescence in vivo. *Photochem Photobiol* 13: 215–224
- Williams JC, Steiner LA and Feher G (1986) Primary structure of the reaction center from *Rhodospirillum rubrum*. *Proteins: Structure, Function and Genetics* 1: 312–325
- Woodbury NWT and Parson WW (1984) Nanosecond fluorescence from isolated photosynthetic reaction centers of *Rhodospirillum rubrum*. *Biochim Biophys Acta* 767: 315–361